H_∞ Tracking Control of Non-lower Triangular Nonlinear Systems: Coronary Artery System

El khaloufi Ghizlane[1,*], *Chaibi* Noreddine[1], *Belamfedel Alaoui* Sadek[2], *Boumhidi* Ismail[1], and *Darouiche* Fatima Zahra[1]

[1]LISAC Laboratory, Faculty of Sciences Dhar el Mahraz, Sidi Mohamed Ben Abdellah University, Fes, 30000, Morocco

[2]College of Computing, University Mohammed VI Polytechnic, Ben Guerir 43150, Morocco

Abstract. This work presents a novel control approach that integrates backstepping and dynamic surface control techniques to design an H_∞ tracking control system. Our focus is on a particular class of nonlinear systems that do not possess lower triangular structure, with a specific application to the coronary system. By employing dynamic surface control, the issue of differential explosion encountered during the backstepping process is effectively addressed, while also guaranteeing robustness. Finally, simulation of coronary artery system proves the effectiveness of the proposed control strategy.

Key Words: H_∞ Control, Coronary Artery System, Backstepping Technique, Dynamic Surface Control.

1 Introduction

The coronary artery system (CAS) plays a pivotal role in maintaining stable heart function, as any sudden pressure variations or occlusions can give rise to arrhythmias, characterized by chaotic blood vessel behavior, resulting in fast, slow, or irregular heart rhythms. This intricate system is subject to fluctuations in inner pressure and diameter, influenced by various unpredictable factors such as heart ectopic pacemakers, thyroid disease, high blood pressure, dynamic irregularities, and heart valve issues. The integrity of a healthy coronary artery vessel is paramount in restraining arrhythmias; failure to do so can culminate in cardiac arrest and even mortality. Given the profound impact of this system on overall health, much research has been devoted to it.

In 1986, [1] introduced a mathematical model for the coronary artery system along with key parameter values, establishing mathematically that coronary artery spasm embodies a nonlinear chaotic system. Acknowledging the susceptibility of chaotic systems to initial conditions or disturbances, which can potentially result in catastrophic chaos within a coronary artery, controlling this system becomes imperative to prevent myocardial infarction [2]. As shown in [3] and [4], the ability to employ minor disturbances to control the cardiac chaos and restore normal cardiac function when deviations occur holds promise to avoid coronary artery spasm.

*e-mail: ghizlane.elkhaloufi@usmba.ac.ma

The field of non-linear control has garnered significant attention, leading to the development of numerous control strategies aimed at tackling non-linear dynamics. These approaches encompass adaptive control methods [5, 6], sliding mode control techniques [7, 8], and T-S fuzzy control strategies [9, 10]. Additionally, the backstepping method, as introduced by Kokotovic [11], has been employed to address the intricate control challenges posed by nonlinear systems. A plethora of results have emerged from this research endeavor, as documented in [12–20]. Nonetheless, it is crucial to recognize two inherent limitations associated with the backstepping control method. Firstly, the complexity of control design and stability analysis undergoes exponential growth when applied to nonlinear systems of lower non-triangular form, a phenomenon commonly called "complexity explosion" in this context. Secondly, backstepping control exhibits sensitivity to measurement noise, which can adversely affect its performance for interconnected systems.

On the side of complexity explosion problem, Swaroop et al. [21] introduced a dynamic surface control (DSC) technique. This approach integrated a low-pass filter was in each control input, which has the advantage of zeroing the derivatives of the virtual control inputs. Thus, it eliminates expansions of differential elements, and consequently reduces controller complexity. On the other side, H_∞ robust control stands as an effective method to achieve stabilization with guaranteed performance. In this context, [22], studied H_∞ control problem to synchronize CAS with it nominal system subjected to disturbances and input delay. Li et al. [23] investigated H_∞ control for CAS via free-matrix-based integral inequality with time-delay. The authors in [24] considered the CAS for H_∞ synchronization problems with input time-varying delay and input disturbances.

Given the CAS imperative need for a control approach capable of surmounting the complexity explosion challenge while concurrently demonstrating robustness, the motivation behind this paper lies in the development of a robust H_∞ tracking control synergized with dynamic surface control.

To address the limitations associated with backstepping, including complexity explosion and sensitivity to measurement errors (Section 2), this paper presents a novel robust H_∞ tracking controller design approach for systems characterized by lower non-triangular form (Section 3), specifically focusing on the coronary artery system. This method combines dynamic surface and backstepping control techniques. Compared to existing findings, the proposed controller scheme effectively eliminates the need for repeated differentiation of virtual controls, all while establishing a robust H_∞ performance metric. Illustrative simulations are provided for the coronary artery system (Section 4). Finally, we present a conclusion with the research line for expected future works (Section 5).

2 Problem formulation and preliminaries

2.1 System description

Consider the general class of the coronary artery system defined by,

$$\begin{cases} \dot{x}_i = f_i(x_1, x_2, \ldots, x_n) + x_{i+1} + \Delta_i, \quad i = 1, 2, \ldots, n-1, \\ \dot{x}_n = g_n(x_1, x_2, \ldots, x_n)\, u + f_n(x_1, x_2, \ldots, x_n) + \Delta_n, \\ y = x_1 \end{cases} \tag{1}$$

where $x_i \in \mathbb{R}, i = \{1, \ldots, n\}$ are the system states; $u(t) \in \mathbb{R}$ and $y(t) \in \mathbb{R}$ represent the system input and output signals, respectively; $f_i(.)$ is known nonlinear function; $g_n(\cdot)$ is a continuous function and satisfies $g_n(\cdot) \neq 0$; Δ_i is bounded disturbances. It is possible to recover the case

Table 1: System parameters [25]

Parameter	b	c	λ	ω	E
Value	0.15	-1.7	-0.65	1	0.3

of the coronary artery system adopted in [25], by specifying $x \in \mathbb{R}^2$, with x_1 and x_2 are the inner diameter changes and the pressure of coronary artery vessel of CAS, respectively;

$$\begin{aligned} f_1(x_1, x_2) &= -bx_1(t) - cx_2(t) + x_2(t), \\ f_2(x_1, x_2) &= -(b+1)\lambda x_1(t) - (c+1)\lambda x_2(t) + \lambda x_1^3(t) + E\cos(\omega t), \\ g_2(x_1, x_2) &= 1, \end{aligned} \tag{2}$$

the control input $u(t)$ is the potency or dosage of the single and double nitrate isosorbide nitrate (isosorbide mononitrate and dinitrate) or the nitroglycerin used for treating angina and other diseases; Δ_1 stands for the uncertainty from the vessel in radius; and Δ_2 describes the uncertainty from the pressure change of the vessel. Figure 1 illustrates the healthy CAS and disease CAS. Additional parameters are given in Table 1.

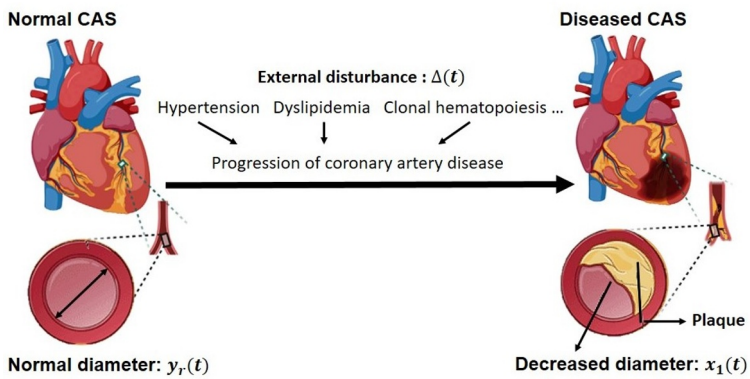

Figure 1: Presentation of healthy CAS and disease CAS

2.2 Objectives

The medical objective is oriented towards achieving synchronization between the states of a Coronary Artery Disease (CAD) system and those of a healthy vessel. To this end, the primary aim of the present study is to formulate a controller design such that the output y (pertaining to the CAD system) effectively tracks a reference signal y_r (generated by the dynamics of a normal CAS). This pursuit also entails achieving an H_∞ performance index γ, which quantifies the extent of disturbance attenuation. The formal definition of the control objective is as follows:

Definition 1 *[26] The H_∞ tracking problem of system* (1) *is said to be solvable if there exists a state feedback control law u so that the closed-loop system satisfies the following properties:*

1. *The tracking error $s_1(t) = y(t) - y_r(t)$ of the resulting closed-loop system* (1) *is asymptotically stable with $\Delta = 0$;*

2. *Under zero initial conditions, the tracking error $s_1(t)$ satisfies the H_∞ performance index,*

$$J = \int_0^\infty \left(\|s_1\|^2 - \gamma^2 \|\bar{\Delta}\|^2 \right) \mathrm{d}t \leqslant 0, \tag{3}$$

where $\gamma > 0$ is the disturbance attenuation rate and $\bar{\Delta} = [\Delta_1, \Delta_2, \ldots, \Delta_n, \rho_1, \rho_2, \ldots, \rho_n]$.

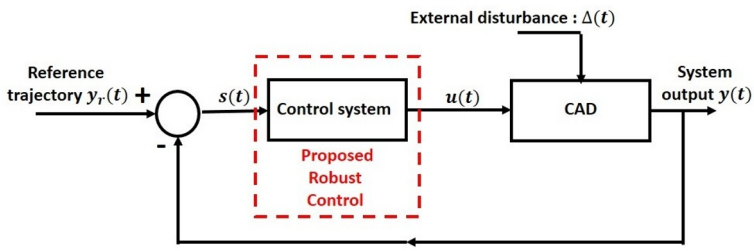

Figure 2: A simplified schematic illustration of the study.

Problem definition

Given the preformance index J in (3), construct a control law u for the dynamic model (1) such as all closed-loop signals are bounded and the output tracking errors converges towards a small neighborhood of zero for all $t \in \mathbb{R}^+$.

2.3 Backstepping method and non-lower triangular nonlinear systems

Why standard back-stepping control approach is not working for CAS?

The conventional back-stepping control methodology encounters limitations when employed for the CAS system defined by Equation (1). In this context, the conventional back-stepping strategy fails to achieve desired outcomes due to the absence of a lower triangular structure within the system, thus impairing its efficacy. Upon employing the standard back-stepping approach, a virtual control law α_{i+1} is derived in each intermediate step ($i = 1, 2, \ldots, n$) to stabilize the ith subsystem. However, complications arise due to the inclusion of the state variable x_n within α_{i+1}, leading to the incorporation of the actual control input u within its derivative. When α_{i+1} is directly injected into the x_{i+1} subsystem, the subsequent virtual control law α_{i+2} becomes inherently contingent on the forthcoming real control input u. This interdependence engenders a cycle of complexity in control law relationships, commonly termed "complexity explosion."

Illustratively, consider a coronary system scenario wherein a pivotal control objective is to facilitate convergence of the tracking error $s_1 = x_1 - y_r$ toward a vicinity of zero. Employing the standard back-stepping methodology, the initial step involves evaluating the time derivative of s_1 as expressed below:

$$\begin{aligned} \dot{s}_1(t) =& \dot{x}_1 - \dot{y}_r, \\ \dot{s}_1(t) =& x_2(t) + f_1(x_1, x_2) - \dot{y}_r, \end{aligned} \tag{4}$$

Suppose we were to design x_2 as $-k_1 s_1 - f_1(x_1, x_2) + \dot{y}_r$. In that case, subsystem (4) could be transformed into $\dot{s}_1(t) = -k_1 s_1$, consequently ensuring asymptotic convergence of the tracking error s_1 to zero. However, as x_2 constitutes a system state variable that cannot be tailored arbitrarily, introducing a virtual control law $\alpha_2 = -k_1 s_1 - f_1(x_1, x_2) + \dot{y}_r$ becomes imperative. The crux of the design objective is to facilitate the convergence of $x_2 - \alpha_2$ to zero. Notably, the presence of x_1 and x_2 within α_2 implies that the derivatives of the nonlinear functions $f_1(x_1, x_2)$ will manifest in the formulation of α_2. Consequently, this intricate interplay leads to the intricate design of the actual control input u if the direct injection of α_2 into the subsequent subsystem ($\dot{s}_2(t) = \dot{x}_2 - \dot{\alpha}_2$) is pursued.

Proposed control approach:

In order to effectively mitigate the challenges posed by the aforementioned complexity explosion, the present study employs a novel approach rooted in the (DSC) technique for control system design. This method entails the utilization of a first-order filter to modulate the virtual control signal α_{i+1}, resulting in the generation of an output signal $\omega(t)$ from the filter. Subsequently, this filtered signal $\omega(t)$ is introduced into the subsequent subsystem. In the culminating stage of this control methodology, specifically the final step denoted as step n, a tangible control law $u(t)$ is meticulously devised to achieve the stabilization of the n subsystems.

Without loss of generality, the proposed approach relies on following technical assumptions.

Assumption 1 *For every $i \in 1, \ldots, n$, the functions f_i and g_i are bounded and $n - i$ times continuously differentiable.*

Assumption 2 *For all $i = 1, 2, \ldots, n$, the functions g_i are invertible.*

Assumption 3 *The desired trajectory y_r is a known and bounded function with time, and its derivatives are also known and bounded.*

3 H_∞ robust controller design

In this section, a backstepping based DSC design scheme is established for the general form of coronary artery system (1), will be devised. Firstly, define the desired trajectory as $y_r(t)$, so the output tracking error is $s_1(t) = y(t) - y_r(t)$. Introducing the following coordinate transformation:

$$s_i(t) = x_i(t) - \omega_i(t), i = 2, \ldots, n, \tag{5}$$

where $\omega_i(t)$ represents the output signal of the low-pass filter with $\alpha_i(t)$ as the input signal, and meets:

$$\begin{cases} \tau_i \dot{\omega}_i(t) + \omega_i(t) = \alpha_i(t), \\ i = 2, \ldots, n, \end{cases} \tag{6}$$

where τ_i is a filtering parameter.
The approximation error of above filters are determined by

$$\rho_i = \omega_i - \alpha_i, i = 2, \ldots, n. \tag{7}$$

The implementation of the control algorithm is provided by the following Theorem 1.

Theorem 1 *Given positive scalars γ, Γ_1, k_i, with $\Gamma_1 = 1/\gamma^2 + 1/2$, if the following virtual control laws satisfy:*

$$\begin{aligned}\alpha_2 =& -k_1 s_1 - \Gamma_1 s_1 - f_1(x_1, x_2, \ldots, x_n) - \frac{s_1}{2\gamma^2} + \dot{y}_r,\\ \alpha_{i+1} =& -k_i s_i - \frac{s_i}{\gamma^2} - f_i(x_1, x_2, \ldots, x_n) - s_{i-1} - \left(\frac{s_i}{2\gamma^2} - \dot{\omega}_i\right),\ \ i = 2, \ldots, n-1,\end{aligned} \tag{8}$$

and actual control law satisfies:

$$u = -\frac{1}{g_n(x_1, x_2, \ldots, x_n)}\left(k_n s_n + \frac{s_n}{\gamma^2} + f_n(x_1, x_2, \ldots, x_n) + s_{n-1} - \dot{\omega}_n\right), \tag{9}$$

then, the system described in (1) *is asymptotically stable and meets the H_∞ performance. All signals are bounded in the closed loop system, and output tracking error can converge to a small neighborhood.*

Next, the sufficiency of the Theorem 1 is proved in the following, and the whole process of proof includes n steps.

Proof 1 ***Step 1:*** *With the aid of $s_1 = x_1 - y_r$, its derivative is given by*

$$\dot{s}_1 = \dot{x}_1 - \dot{y}_r = f_1(x_1, x_2, \ldots, x_n) + x_2 + \Delta_1 - \dot{y}_r. \tag{10}$$

Choose the following Lyapunov function:

$$V_1(s_1) = \frac{1}{2}s_1^2 \tag{11}$$

Define the following function:

$$P_1 = \frac{1}{2}s_1^2 - \frac{\gamma^2}{2}\Delta_1^2 + \dot{V}_1(s_1). \tag{12}$$

Substituting the derivative of $V_1(s_1)$, $x_2 = s_2 + \omega_2$, and $\omega_2 = \rho_2 + \alpha_2$ into (12)*, we obtain*

$$\begin{aligned}P_1 =& \frac{1}{2}s_1^2 - \frac{\gamma^2}{2}\Delta_1^2 + s_1(f_1(x_1, \ldots, x_n) + x_2 - \dot{y}_r + \Delta_1) \qquad (13)\\ =& -\frac{1}{4}\gamma^2\Delta_1^2 - \left(\frac{\gamma}{2}\Delta_1 - \frac{s_1}{\gamma}\right)^2 + s_1(\Gamma_1 s_1 + f_1(x_1, \ldots, x_n) + s_2 + \rho_2 + \alpha_2 - \dot{y}_r)\\ \leqslant& -\frac{1}{4}\gamma^2\Delta_1^2 - \left(\frac{\gamma}{2}\Delta_1 - \frac{s_1}{\gamma}\right)^2 + s_1 s_2 + \frac{s_1^2}{2\gamma^2} + \frac{\gamma^2}{2}\rho_2^2 + s_1(\Gamma_1 s_1 + f_1(x_1, \ldots, x_n) + \alpha_2 - \dot{y}_r),\end{aligned}$$

where $\Gamma_1 = 1/\gamma^2 + 1/2$, and the inequality above is obtained by using the following relation:

$$s_1\rho_2 \leqslant \frac{s_1^2}{2\gamma^2} + \frac{\gamma^2}{2}\rho_2^2. \tag{14}$$

Introduce the virtual control α_2 as follows:

$$\alpha_2 = -k_1 s_1 - \Gamma_1 s_1 - f_1 - \frac{s_1}{2\gamma^2} + \dot{y}_r, \tag{15}$$

where k_1 is a positive design parameter. It follows from substituting α_2 into (13) *that*

$$P_1 \leqslant -\frac{1}{4}\gamma^2\Delta_1^2 - \left(\frac{\gamma}{2}\Delta_1 - \frac{s_1}{\gamma}\right)^2 - k_1 s_1^2 + s_1 s_2 + \frac{\gamma^2}{2}\rho_2^2. \tag{16}$$

Step 2: *It is easily obtained that*

$$\dot{s}_2 = \dot{x}_2 - \dot{\omega}_2 = f_2(x_1, x_2, \ldots, x_n) + x_3 + \Delta_2 - \dot{\omega}_2. \tag{17}$$

Select a Lyapunov function candidate:

$$V_2(s_1, s_2) = V_1(s_1) + \frac{1}{2}s_2^2 \tag{18}$$

By differentiating both sides of (18)*, the following relation can be obtained:*

$$\dot{V}_2(s_1, s_2) = \dot{V}_1(s_1) + s_2\dot{s}_2. \tag{19}$$

Substituting (12) *into the equation above gives*

$$\dot{V}_2(s_1, s_2) = P_1 - \frac{1}{2}s_1^2 + \frac{\gamma^2}{2}\Delta_1^2 + s_2\dot{s}_2. \tag{20}$$

Define the following function:

$$P_2 = \frac{1}{2}s_1^2 - \frac{\gamma^2}{2}\sum_{j=1}^{2}\left(\Delta_j^2 + \rho_j^2\right) + \dot{V}_2(s_1, s_2). \tag{21}$$

Then, by substituting (20) *into* (21) *and taking* (16) *into consideration, it follows that*

$$\begin{aligned} P_2 =& -\frac{\gamma^2}{2}\Delta_2^2 - \frac{\gamma^2}{2}\rho_2^2 + P_1 + s_2\dot{s}_2 \\ \leqslant& \Phi_1 - \frac{\gamma^2}{4}\Delta_2^2 - \left(\frac{\gamma}{2}\Delta_2 - \frac{s_2}{\gamma}\right)^2 + s_2\left(\frac{s_2}{\gamma^2} + f_2(x_1, \ldots, x_n) + x_3 + s_1 - \dot{\omega}_2\right), \end{aligned} \tag{22}$$

where $\Phi_1 = -\frac{1}{4}\gamma^2\Delta_1^2 - \left(\frac{\gamma}{2}\Delta_1 - \frac{s_1}{\gamma}\right)^2 - k_1 s_1^2$. *Substituting* $x_3 = s_3 + \omega_3$ *and* $\omega_3 = \rho_3 + \alpha_3$ *into* (22) *produces*

$$\begin{aligned} P_2 \leqslant& \Phi_1 - \frac{1}{4}\gamma^2\Delta_2^2 - \left(\frac{\gamma}{2}\Delta_2 - \frac{s_2}{\gamma}\right)^2 + s_2\left(\frac{s_2}{\gamma^2} + f_2(x_1, \ldots, x_n) + s_3 + \rho_3 + \alpha_3\right) + s_2(s_1 - \dot{\omega}_2) \\ \leqslant& \Phi_1 - \frac{\gamma^2}{4}\Delta_2^2 - \left(\frac{\gamma}{2}\Delta_2 - \frac{s_2}{\gamma}\right)^2 + s_2\left(\frac{s_2}{\gamma^2} + f_2(x_1, \ldots, x_n) + \alpha_3 + s_3\right) \\ &+ \frac{s_2^2}{2\gamma^2} + \frac{\gamma^2}{2}\rho_3^2 + s_2(s_1 - \dot{\omega}_2), \end{aligned} \tag{23}$$

where the inequality is obtained by using the following relation:

$$s_2\rho_3 \leqslant \frac{s_2^2}{2\gamma^2} + \frac{\gamma^2}{2}\rho_3^2. \tag{24}$$

Define the virtual control α_3 as follows:

$$\alpha_3 = -k_2 s_2 - \frac{s_2}{\gamma^2} - f_2(x_1, \ldots, x_n) - s_1 - \frac{s_2}{2\gamma^2} + \dot{\omega}_2, \tag{25}$$

where k_1 is a positive design parameter. It follows from substituting α_3 into (23) *that*

$$P_2 \leqslant \Phi_1 - \frac{\gamma^2}{4}\Delta_2^2 - \left(\frac{\gamma}{2}\Delta_2 - \frac{s_2}{\gamma}\right)^2 - k_2 s_2^2 + s_2 s_3 + \frac{\gamma^2}{2}\rho_3^2. \tag{26}$$

Step i *$i(i = 3, \ldots, n-1)$: Suppose that at Step $i-1$, the function*

$$P_{i-1} = \frac{1}{2}s_1^2 - \frac{\gamma^2}{2}\sum_{j=1}^{i-1}\left(\Delta_j^2 + \rho_j^2\right) + \dot{V}_{i-1}(s_1, \ldots, s_{i-1}) \tag{27}$$

satisfies the inequality

$$P_{i-1} \leqslant \Phi_1 - \sum_{j=2}^{i-1}\left[\frac{\gamma^2}{4}\Delta_j^2 + \left(\frac{\gamma}{2}\Delta_j - \frac{s_j}{\gamma}\right)^2\right] - \sum_{j=2}^{i-1} k_j s_j^2 + s_{i-1}s_i + \frac{\gamma^2}{2}\rho_i^2, \tag{28}$$

where

$$V_{i-1}(s_1, \ldots, s_{i-1}) = V_{i-2}(s_1, \ldots, s_{i-2}) + \frac{1}{2}s_{i-1}^2. \tag{29}$$

Consider the i th subsystem

$$\dot{s}_i = \dot{x}_i - \dot{\omega}_i = f_i(x_1, x_2, \ldots, x_n) + x_{i+1} + \Delta_i - \dot{\omega}_i. \tag{30}$$

The following Lyapunov function candidate:

$$V_i(s_1, \ldots, s_i) = V_{i-1}(s_1, \ldots, s_{i-1}) + \frac{1}{2}s_i^2. \tag{31}$$

By differentiating both sides of (31)*, the following can be obtained:*

$$\dot{V}_i(s_1, \ldots, s_i) = \dot{V}_{i-1}(s_1, \ldots, s_{i-1}) + s_i\dot{s}_i \tag{32}$$

Substituting (29) *and* (27) *into the equation above yields*

$$\dot{V}_i(s_1, \ldots, s_i) = P_{i-1} - \frac{1}{2}s_1^2 + \frac{\gamma^2}{2}\sum_{j=1}^{i-1}\left(\Delta_j^2 + \rho_j^2\right) + s_i\dot{s}_i. \tag{33}$$

Define the function

$$P_i = \frac{1}{2}s_1^2 - \frac{\gamma^2}{2}\sum_{j=1}^{i}\left(\Delta_j^2 + \rho_j^2\right) + \dot{V}_i(s_1, \ldots, s_i). \tag{34}$$

Then, by using (33) *and* (28)*, it can be easily verified that*

$$\begin{aligned} P_i =& \frac{1}{2}s_1^2 - \frac{\gamma^2}{2}\sum_{j=1}^{i}\left(\Delta_j^2 + \rho_j^2\right) + P_{i-1} - \frac{1}{2}s_1^2 + \frac{\gamma^2}{2}\sum_{j=1}^{i-1}\left(\Delta_j^2 + \sigma_j^2\right) + s_i\dot{s}_i \\ \leqslant& \Phi_1 - \sum_{j=2}^{i}\left[\frac{\gamma^2}{4}\Delta_j^2 + \left(\frac{\gamma}{2}\Delta_j - \frac{s_j}{\gamma}\right)^2\right] - \sum_{j=2}^{i-1} k_j s_j^2 \\ &+ s_i\left(\frac{s_i}{\gamma^2} + f_i(x_1, x_2, \ldots, x_n) + x_{i+1} + s_{i-1} - \dot{\omega}_i\right). \end{aligned} \tag{35}$$

Substituting $x_{i+1} = s_{i+1} + \omega_{i+1}$ *and* $\omega_{i+1} = \rho_{i+1} + \alpha_{i+1}$ *into* (35) *gives*

$$\begin{aligned} P_i \leqslant & \Phi_1 - \sum_{j=2}^{i}\left[\frac{\gamma^2}{4}\Delta_j^2 + \left(\frac{\gamma}{2}\Delta_j - \frac{s_j}{\gamma}\right)^2\right] - \sum_{j=2}^{i-1} k_j s_j^2 + s_i s_{i+1} + s_i\rho_{i+1} \\ & + s_i\left(\frac{s_i}{\gamma^2} + f_i\left(x_1,\ldots,x_n\right) + \alpha_{i+1} + s_{i-1} - \dot{\omega}_i\right) \\ \leqslant & \Phi_1 - \sum_{j=2}^{i}\left[\frac{\gamma^2}{4}\Delta_j^2 + \left(\frac{\gamma}{2}\Delta_j - \frac{s_j}{\gamma}\right)^2\right] - \sum_{j=2}^{i-1} k_j s_j^2 + s_i s_{i+1} + \frac{\gamma^2}{2}\rho_{i+1}^2 \\ & + s_i\left(\frac{s_i}{\gamma^2} + f_i\left(x_1,\ldots,x_n\right) + \alpha_{i+1} + s_{i-1}\right) + s_i\left(\frac{s_i}{2\gamma^2} - \dot{\omega}_i\right) \end{aligned} \tag{36}$$

where the inequality is obtained by

$$s_i\rho_{i+1} \leqslant \frac{s_i^2}{2\gamma^2} + \frac{\gamma^2}{2}\rho_{i+1}^2. \tag{37}$$

Design the virtual control α_{i+1} *as follows:*

$$\alpha_{i+1} = -k_i s_i - \frac{s_i}{\gamma^2} - f_i\left(x_1,\ldots,x_n\right) - s_{i-1} - \left(\frac{s_i}{2\gamma^2} - \dot{\omega}_i\right), \tag{38}$$

where k_i *is a positive design parameter. It follows from substituting* α_{i+1} *into* (36) *that*

$$P_i \leqslant \Phi_1 - \sum_{j=2}^{i}\left[\frac{\gamma^2}{4}\Delta_j^2 + \left(\frac{\gamma}{2}\Delta_j - \frac{s_j}{\gamma}\right)^2\right] - \sum_{j=2}^{i} k_j s_j^2 + s_i s_{i+1} + \frac{\gamma^2}{2}\rho_{i+1}^2. \tag{39}$$

Step n: *Repeating step similar to step i, the following equation is satisfied*

$$\dot{s}_n = \dot{x}_n - \dot{\omega}_n = f_n\left(x_1, x_2, \ldots, x_n\right) + g_n\left(x_1, x_2, \ldots, x_n\right)u + \Delta_n - \dot{\omega}_n. \tag{40}$$

Select Lyapunov function candidate as follows

$$V_n\left(s_1,\ldots,s_n\right) = V_{n-1}\left(s_1,\ldots,s_{n-1}\right) + \frac{1}{2}s_n^2. \tag{41}$$

The following relation can be obtained by differentiating both sides of (39) *and using* (41) *with* $i = n-1$ *:*

$$\begin{aligned} \dot{V}_n\left(s_1,\ldots,s_n\right) &= \dot{V}_{n-1}\left(s_1,\ldots,s_{n-1}\right) + s_n\dot{s}_n \\ &= P_{n-1} - \frac{1}{2}s_1^2 + \frac{\gamma^2}{2}\sum_{j=1}^{n-1}\left(\Delta_j^2 + \rho_j^2\right) + s_n\dot{s}_n. \end{aligned} \tag{42}$$

Define the following function:

$$P_n = \frac{1}{2}s_1^2 - \frac{\gamma^2}{2}\sum_{j=1}^{n}\left(\Delta_j^2 + \rho_j^2\right) + \dot{V}_n\left(s_1,\ldots,s_n\right). \tag{43}$$

Then, by using (42) *and* (43)*, it can be easily verified that*

$$\begin{aligned} P_n =& \frac{1}{2}s_1^2 - \frac{\gamma^2}{2}\sum_{j=1}^{n}\left(\Delta_j^2+\rho_j^2\right) + P_{n-1} - \frac{1}{2}s_1^2 + \frac{\gamma^2}{2}\sum_{j=1}^{n-1}\left(\Delta_j^2+\rho_j^2\right) + s_n\dot{s}_n \\ \leqslant& -\frac{\gamma^2}{2}\Delta_n^2 - \frac{\gamma^2}{2}\rho_n^2 + \Phi_1 - \sum_{j=2}^{n-1}\left[\frac{\gamma^2}{4}\Delta_j^2 + \left(\frac{\gamma}{2}\Delta_j - \frac{s_j}{\gamma}\right)^2\right] - \sum_{j=2}^{n-1}k_j s_j^2 \\ &+ s_{n-1}s_n + \frac{\gamma^2}{2}\rho_n^2 + s_n\left(f_n\left(x_1,\ldots,x_n\right) + g\left(x_1,\ldots,x_n\right)u + \Delta_n - \dot{\omega}_n\right) \\ \leqslant& \Phi_1 - \sum_{j=2}^{n}\left[\frac{\gamma^2}{4}\Delta_j^2 + \left(\frac{\gamma}{2}\Delta_j - \frac{s_j}{\gamma}\right)^2\right] - \sum_{j=2}^{n-1}k_j s_j^2 \\ &+ s_n\left(\frac{s_n}{\gamma^2} + f_n\left(x_1,\ldots,x_n\right) + g\left(x_1,\ldots,x_n\right)u + s_{n-1} - \dot{\omega}_n\right). \end{aligned} \tag{44}$$

Choose the control input u as follows:

$$u = -\frac{1}{g\left(x_1,x_2,\ldots,x_n\right)}\left(k_n s_n + \frac{s_n}{\gamma^2} + f_n\left(x_1,x_2,\ldots,x_n\right) + s_{n-1} - \dot{\omega}_n\right), \tag{45}$$

where k_i is a positive design parameter. It follows from substituting u into (43) *that*

$$P_n \leqslant \Phi_1 - \sum_{j=2}^{n}\left[\frac{\gamma^2}{4}\Delta_j^2 + \left(\frac{\gamma}{2}\Delta_j - \frac{s_j}{\gamma}\right)^2\right] - \sum_{j=2}^{n}k_j s_j^2 \leq 0. \tag{46}$$

Select $V_N\left(s_1,\ldots,s_n\right) = 2V_n\left(s_1,\ldots,s_n\right)$. Then it follows from (43) *that the derivative of V_N satisfies*

$$\dot{V}_N\left(s_1,\ldots,s_n\right) = 2P_n - \left(\|s_1\|^2 - \gamma^2\|\Delta\|^2 - \gamma^2\|\rho\|^2\right). \tag{47}$$

Because of $P_n \leq 0$, the following inequality is obtained:

$$\dot{V}_N\left(s_1,\ldots,s_n\right) \leq \left(\gamma^2\|\bar{\Delta}\|^2 - \|s_1\|^2\right). \tag{48}$$

By integrating both sides of inequality (48)*, inequality* (3) *in Definition 1 can be obtained, which indicates that the L_2 gain from uncertainties $\bar{\Delta}_i$ to output s_1 is smaller than or equal to a positive constant γ.*

So far, the tracking control design has been accomplished based on the backsteping algorithm.

4 Simulation results

Simulation studies using MATLAB are performed to verify the tracking effectiveness of the developed controller for coronary artery system (1).
The relevant design parameters are as follows: $\Delta_1 = 0$, $\Delta_2 = 0.3cos(\omega t)$, $y_r = 0.1\cos(3t)$, $k_1 = 9, k_2 = 9$, and $\tau_2 = 0.01, \gamma = 0.5$.
The initial states of the system and of the filter are $x_1(0) = 0$, $x_2(0) = 0.2$ and $\omega_2(0) = 0$.

The block diagram of the design procedure for the proposed controller given in section 3 is shown in Figure 4.

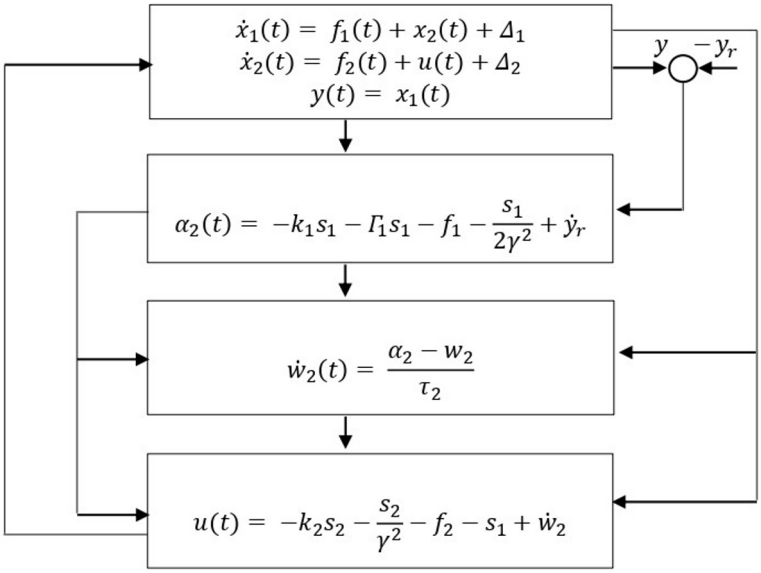

Figure 3: The block diagram of the design procedure for the proposed controller.

The simulation is executed by using the design parameters above, and all the simulation response curves are illustrated in figures 4 - 8. As you can see from figure 4, the system output $y(t)$ follow the reference signal $y_r(t)$ quickly and precisely. figure 5 illustrates the tracking error trajectory. Obviously, it is found that the tracking error can converge to a small neighborhood of zero. The response curves of the states x_1, x_2 and the control law u are illustrated in figure 6 and figure 7, respectively, which illustrate distinctly that all the signals are bounded stable. Figure 8 shows the trajectories of the input and output signals of the first-order low-pass filters. Therefore, it is easy to see that the proposed method can achieve a better performance with small control gains, and the proposed control design scheme is feasible and effective.

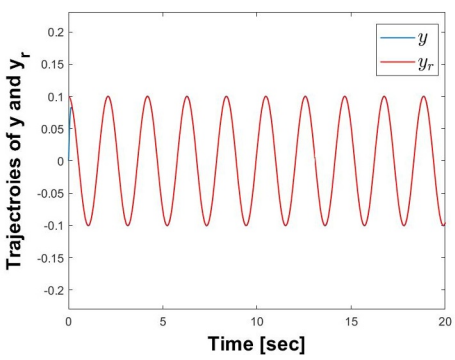

Figure 4: Trajectroies of y and y_r of the proposed method.

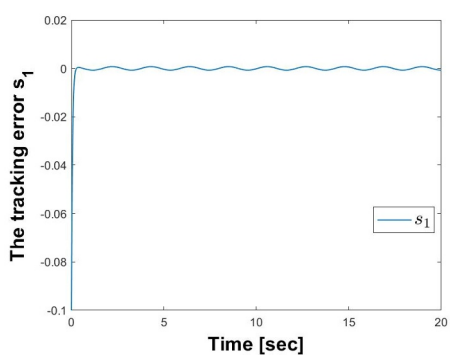

Figure 5: Response curve of the tracking error s_1.

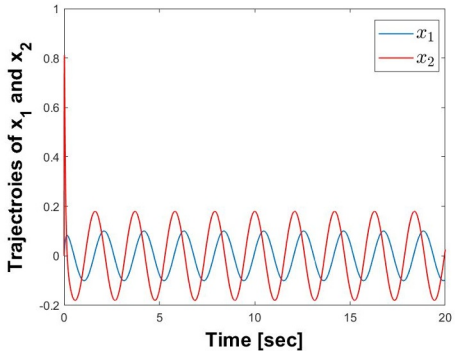

Figure 6: Response curves of x_1 and x_2.

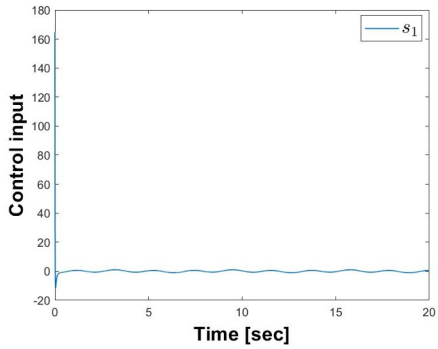

Figure 7: Control input.

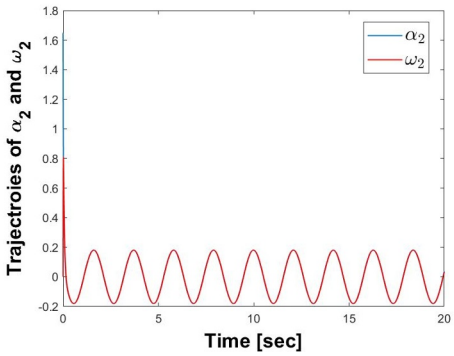

Figure 8: First-order filters.

5 Conclusion

This work formulated a backstepping control strategy tailored to address the complexity explosion and robustness challenges in coronary artery system. Leveraging Dynamic Surface Control and H_∞ guaranteed performance, we have effectively circumvented the need for virtual control differentiation at each recursive step during the backstepping design process while guaranteeing robustness arising from disturbances. The simulation results showed significant enhancements in tracking performance.

For future endeavors, it is worth exploring the integration of neural or fuzzy adaptive control methodologies. These approaches can be instrumental in approximating uncertain terms within the CAS system, further enhancing the control precision and adaptability of our framework.

References

[1] Xu, ZY and Liu, C, The chaos phenomenon of the models for two types of muscular blood vessel, *J. Biomash* **1**, 109–115 (1986).

[2] Garfinkel, Alan and Spano, Mark L and Ditto, William L and Weiss, James N, Controlling cardiac chaos, *Science* **257**, 1230–1235 (1992).

[3] Guo, Jie and Zhao, Zhanshan and Shi, Fengdong and Wang, Ruikun and Li, Shasha, Observer-based synchronization control for coronary artery time-delay chaotic system, *IEEE Access* **7**, 51222–51235 (2019).

[4] Guo, Jie and Zhao, Zhanshan and Zhang, Jing and Ding, Gang, Adaptive observation control for synchronization of coronary artery time-delay systems, *Modern Physics Letters B* **33**, 1950454 (2019).

[5] Li, Hongyi and Bai, Lu and Zhou, Qi and Lu, Renquan and Wang, Lijie, Adaptive fuzzy control of stochastic nonstrict-feedback nonlinear systems with input saturation, *IEEE Transactions on Systems, Man, and Cybernetics: Systems* **47**, 2185–2197 (2017).

[6] Wang, Hui and Zhu, Quanxin, Adaptive output feedback control of stochastic nonholonomic systems with nonlinear parameterization, *Automatica* **98**, 247–255 (2018).

[7] Zhou, Qi and Yao, Deyin and Wang, Jiahui and Wu, Chengwei, Robust control of uncertain semi-Markovian jump systems using sliding mode control method, *Applied Mathematics and computation* **286**, 72–87 (2016).

[8] Ding, Shihong and Mei, Keqi and Li, Shihua, A new second-order sliding mode and its application to nonlinear constrained systems, *IEEE Transactions on Automatic Control* **6**, 2545–2552 (2018).

[9] Marouf, Sepideh and Esfanjani, Reza Mahboobi and Akbari, Ahmad and Barforooshan, Mohsen, T–S fuzzy controller design for stabilization of nonlinear networked control systems, *Engineering Applications of Artificial Intelligence* **50**, 135–141 (2016).

[10] Sakthivel, Rathinasamy and Harshavarthini, S and Kavikumar, Ramasamy and Ma, Yong-Ki, Robust tracking control for fuzzy Markovian jump systems with time-varying delay and disturbances, *IEEE Access* **6**, 66861–66869 (2018).

[11] Kokotovic, PV and Krstic, M and Kanellakopoulos, Ioannis, Backstepping to passivity: recursive design of adaptive systems, *[1992] Proceedings of the 31st IEEE Conference on Decision and Control*, 3276–3280 (1992).

[12] Li, Shi and Ahn, Choon Ki and Guo, Jian and Xiang, Zhengrong, Global output feedback sampled-data stabilization of a class of switched nonlinear systems in the p-normal form, *IEEE Transactions on Systems, Man, and Cybernetics: Systems* **51**, 1075–1084 (2019).

[13] Li, Shi and Guo, Jian and Xiang, Zhengrong, Global stabilization of a class of switched nonlinear systems under sampled-data control, *IEEE Transactions on Systems, Man, and Cybernetics: Systems* **49**, 1912–1919 (2018).

[14] Li, Shi and Ahn, Choon Ki and Xiang, Zhengrong, Sampled-data adaptive output feedback fuzzy stabilization for switched nonlinear systems with asynchronous switching, *IEEE Transactions on Fuzzy Systems* **27**, 200–205 (2018).

[15] Zou, Wencheng and Xiang, Zhengrong, Event-triggered containment control of second-order nonlinear multi-agent systems, *IEEE Transactions on Fuzzy Systems* **356**, 10421–10438 (2019).

[16] Zhao, Xudong and Wang, Xinyong and Zhang, Shuo and Zong, Guangdeng, Adaptive neural backstepping control design for a class of nonsmooth nonlinear systems, *IEEE Transactions on Systems, Man, and Cybernetics: Systems* **49**, 1820–1831 (2018).

[17] Liu, Lei and Liu, Yan-Jun and Tong, Shaocheng, Fuzzy-based multierror constraint control for switched nonlinear systems and its applications, *IEEE Transactions on Fuzzy Systems* **27**, 1519–1531 (2018).

[18] Li, Dapeng and Chen, CL Philip and Liu, Yan-Jun and Tong, Shaocheng, Neural network controller design for a class of nonlinear delayed systems with time-varying full-state constraints, *IEEE transactions on neural networks and learning systems* **30**, 2625–2636

(2019).

[19] Li, Dapeng and Liu, Lei and Liu, Yan-Jun and Tong, Shaocheng and Chen, CL Philip, Adaptive NN control without feasibility conditions for nonlinear state constrained stochastic systems with unknown time delays, *IEEE Transactions on Cybernetics* **49**, 4485–4494 (2019).

[20] Liu, Yan-Jun and Lu, Shumin and Tong, Shaocheng and Chen, Xinkai and Chen, CL Philip and Li, Dong-Juan, Adaptive control-based barrier Lyapunov functions for a class of stochastic nonlinear systems with full state constraints, *Automatica* **49**, 83–93 (2018).

[21] Swaroop, D and Hedrick, J Karl and Yip, Patrick P and Gerdes, J Christian, Dynamic surface control for a class of nonlinear systems, *IEEE transactions on automatic control* **45**, 1893–1899 (2000).

[22] Zhang, Jing and Li, Shasha and Zhao, Zhanshan and Sun, Jie, Improved synchronization criteria for coronary artery input time-delay system, *IEEE Access* **6**, 68221–68232 (2018).

[23] Li, Sha-sha and Zhao, Zhan-shan and Zhang, Jing and Sun, Jie and Sun, Lian-kun, H_∞ Control of Coronary Artery Input Time-Delay System via the Free-Matrix-Based Integral Inequality, *Mathematical Problems in Engineering* **2018**, 1–12 (2018).

[24] Li, Xiao-Meng and Zhao, Zhan-Shan and Zhang, Jing and Sun, Lian-Kun, H_∞ synchronization of the coronary artery system with input time-varying delay, *Chinese Physics B* **25**, 060504 (2016).

[25] Gong, CY and Li, YM and Sun, XH, Backstepping control of synchronization for biomathematical model of muscular blood vessel, *Journal of Applied Sciences* **24**, 604–607 (2006).

[26] Gao, Chuang and Jia, Yufu and Liu, Xiaoping and Chen, Ming, Modeling and prescribed H-infinity tracking control for strict feedback nonlinear systems, *Nonlinear Analysis: Modelling and Control* **22**, 317–333 (2017).